Hindawi

Research Article

Propagation of Partially Coherent Flat-Topped Vortex Hollow Beams in Anisotropic Turbulent Plasma

Abdu A. Alkelly [ID]**, M. A. H. Khaled** [ID]**, and Labiba F. Hassan** [ID]

Physics Department, Faculty of Science, Sana'a University, Sana'a, Yemen

Correspondence should be addressed to Abdu A. Alkelly; aa_alkelly@yahoo.com

The propagation properties of partially coherent circular flat-topped (FT) vortex hollow/nonvortex beams are studied in anisotropic turbulent plasma. The analytical expression of the optical intensity of these beams is obtained by employing the extended Huygens–Fresnel integral. The effects of the source and turbulent plasma parameters on the intensity distribution of partially coherent circular FT vortex hollow/nonvortex beams are analyzed numerically. The results show that partially coherent circular FT vortex hollow/nonvortex beams will finally converge into a Gaussian intensity profile at increasing propagation distances. The results also showed that the partially coherent FT vortex hollow/nonvortex beams with higher coherence are less affected by anisotropic turbulent plasma than the less coherent beams.

1. Introduction

The propagation of laser beams in atmospheric turbulence has received great interest in the past decades because of their applications in remote sensing and free-space optical communication systems [1–3]. On the other hand, hypersonic turbulence (due to turbulence in the flow of a high-speed flight vehicle) is an important factor in understanding optical propagation and optical communication [4].In fact, when an aircraft or spacecraft pierces the Earth's atmosphere with exceedingly high-speed (hypersonic), the gas environment surrounding the hypersonic aircraft will rub against the aircraft body causing a hypersonic plasma sheath to surround the aircraft. Many experiments have confirmed that such a plasma sheath has anisotropic turbulence properties [5, 6]. The presence of anisotropic turbulent plasma sheaths around the vehicles can have a strong influence on the communication characteristics between the vehicles and radars. It can perturb communication and in some circumstances may lead to a disconnection [7, 8].In recent years, the propagation of various laser beams in anisotropic turbulent plasma has been investigated extensively [9–13].

Vortices are defined as phase singularities because they consist of a dark center and a spiraling phase front, where the phase is indefinite in the center. In 1992, Allen et al. [14] proved that a vortex beam can carry an orbital angular momentum (OAM). Due to the perpendicularity and completeness of OAM, the OAM has infinite-dimensional Hilbert space and can carry infinite-dimensional information, so it allows for an increase in the channel transmission capacity. Thus, it has been widely used in optical communication systems in free space and turbulent environments [15].

In 1994, Gori [16] found the flat-topped beam is derived from the fundamental Gaussian beam by introducing an order of flatness parameter. In medical applications and many practical applications, such as material processing and inertial confinement fusion, the flat-topped spatial beam profile is often required. When the flat-topped beam passes through a spiral phase plate, it becomes a flat-topped vortex hollow beam [17, 18]. The phase of the flat-topped vortex hollow beam can be adjusted by the spiral phase plate. The main advantages of the flat-topped vortex hollow beam are that it carries the orbital angular momentum that has many applications in atomic optics, and the flat-topped vortex
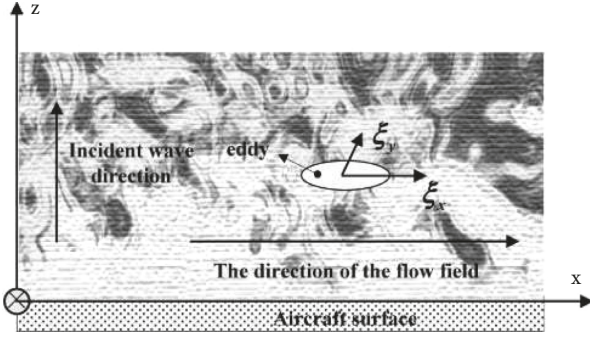
Figure 1: Sketch of hypersonic turbulence (figure from [24]).

hollow beam keeps the dark hollow spot in the far field; these can expand beam applications such as long-distance stealth detection and invisible control. Very recently, some studies have been conducted on the propagation of the partially coherent FT beam and partially coherent flat-topped vortex hollow beam [19–23].

To the best of our knowledge, there are no detailed investigations on the propagation of vortex hollow/non-vortex of a partially coherent circular FT beam in anisotropic turbulent plasma. This paper is devoted to studying the beam evolution properties through anisotropic turbulent plasma based on the extended Huygens–Fresnel formula, and the analytical expressions for the intensity are derived. We will focus our studies on the effects of the source and turbulent plasma parameters on the intensity distribution, beam width and beam quality, and the comparison of the intensity distribution versus the propagation distance between partially coherent circular flat-topped vortex hollow and nonvortex beams in anisotropic turbulent plasma.

2. The Wave Structure Function through the Anisotropic Turbulent Plasma

The wave structure function describing a spherical wave propagating in anisotropic turbulent plasma is shown in Figure 1 and can be expressed as [24]

$$
\begin{aligned}
D_\psi\left(\mathbf{r}_1' - \mathbf{r}_2'\right) = {} & 8\pi^2 k^2 z \int_0^1 \mathrm{d}\xi \int_0^\infty \mathrm{d}\kappa\kappa\Phi_n(\kappa) \\
& \left[1 - J_0\left(\kappa\left|(1-\xi)(\mathbf{r}_1 - \mathbf{r}_2) + \xi(\mathbf{r}_1' - \mathbf{r}_2')\right|\right)\right], \\
\simeq {} & 2D_{sp}(z)\left[(\mathbf{r}_1 - \mathbf{r}_2)^2 + (\mathbf{r}_1 - \mathbf{r}_2)(\mathbf{r}_1' - \mathbf{r}_2') + (\mathbf{r}_1' - \mathbf{r}_2')^2\right],
\end{aligned}
\tag{1}
$$

where

$$
D_{sp}(z) = \frac{\pi^2 k^2 z}{3} \int_0^\infty \kappa^3 \Phi_n(\kappa)\mathrm{d}\kappa,
\tag{2}
$$

where $k = 2\pi/\lambda$ is the wave number, in which λ is the incident wavelength and z is the beam propagation distance. $D_{sp}(z) = 1/\rho_0^2(z)$, in which $\rho_0(z)$ is the coherence length of a spherical wave propagation in anisotropic turbulent

plasma, $\kappa \equiv (\kappa_x, \kappa_y)$ is the transverse spatial frequency, and $\Phi_n(\kappa)$ is the anisotropic refractive index power spectrum of turbulent plasma being transformed from the modified von Karman spectrum and is expressed as follows [25]:

$$
\Phi_n(\kappa) = a_1 \frac{64\pi\langle n_1^2\rangle L_0^2 (m_1 - 1)}{\left(1 + 100\kappa L_0^2\right)^{m_1}} \exp\left(-\frac{\kappa}{\kappa_0}\right),
\tag{3}
$$

where $\langle n_1^2\rangle$ is the variance of the refractive index fluctuation, m_1 is a constant $m_1 = 4 - d, d$ is the fractal dimension of the anisotropic turbulent plasma, and L_0 is the outer scale of anisotropic turbulent plasma. Here, a_1 is a fitting parameter, which can be expressed as $a_1 = 475(\kappa_0)^{2m_1}$ where $\kappa_0 = (2\pi/l_0)^{m_1 - 0.7}$ in which l_0 represents the inner scale of anisotropic turbulent plasma. The relation between L_0 and l_0 can be expressed as follows [26]:

$$
\frac{L_0}{l_0} = R_e^{(3/4)},
\tag{4}
$$

where R_e represents the Reynolds number. For the fully developed turbulence in the mixing layer, $R_e = 5 \times 10^5$, $d = 2.6$, and $m_1 = 1.4$. If the outer scale $L_0 = 0.1m$, then the inner scale $l_0 = 5.3 \times 10^{-6}m$. Considering the large-scale asymmetric structure of turbulence eddies on the path, the anisotropic spectrum can be expressed as follows [24]:

$$
\Phi_n(\kappa') = a_1 \frac{64\pi\langle n_1^2\rangle L_0^2 (m_1 - 1)}{\left(1 + 100\kappa L_0^2\right)^{m_1}} \exp\left(-\frac{\kappa}{\kappa_0'}\right),
\tag{5}
$$

where $\kappa' = |\kappa'| = \sqrt{\xi_x^2 \kappa_x^2 + \xi_y^2 \kappa_y^2 + \kappa_z^2}$ will be isotropic in the stretched wave number space $\kappa' = (\kappa_x', \kappa_y', \kappa_z')$, $\kappa_x' = \xi_x \kappa_x$, $\kappa_y' = \xi_y \kappa_y$, $\kappa_z' = \kappa_z$, and ξ_x and ξ_y are two anisotropy parameters representing scale-dependent stretching along the x and y direction, respectively. It is noted that when $\xi_x = \xi_y = 1$, Equation (5) reduces itself to isotropic power spectrum Equation (3). Substituting Equation (5) into Equation (2) and applying the Markov approximation, we obtain

$$
\begin{aligned}
D_{sp}(z) = {} & \frac{32\pi^3 k^2 z a_1 \langle n_1^2\rangle L_0^2 (m_1 - 1)}{3} \frac{\left(\xi_x^2 + \xi_y^2\right)}{\xi_x^3 \xi_y^3} \left(\frac{1}{100 L_0^2}\right)^4 \\
& U\left(4, 5 - m_1, \frac{1}{100 L_0^2 \kappa_0}\right) \times \Gamma(4),
\end{aligned}
\tag{6}
$$

where $U(a, b, z)$ is the confluent hypergeometric function of the second kind and $\Gamma(\cdot)$ is the gamma function.

3. The Partially Coherent Flat-Topped Vortex Hollow Beam of Circular Symmetry in Anisotropic Turbulent Plasma

In the Cartesian coordinate system, the electric field of a circular flat-topped vortex hollow beam at the source plane $(z = 0)$ is expressed as follows [17]:
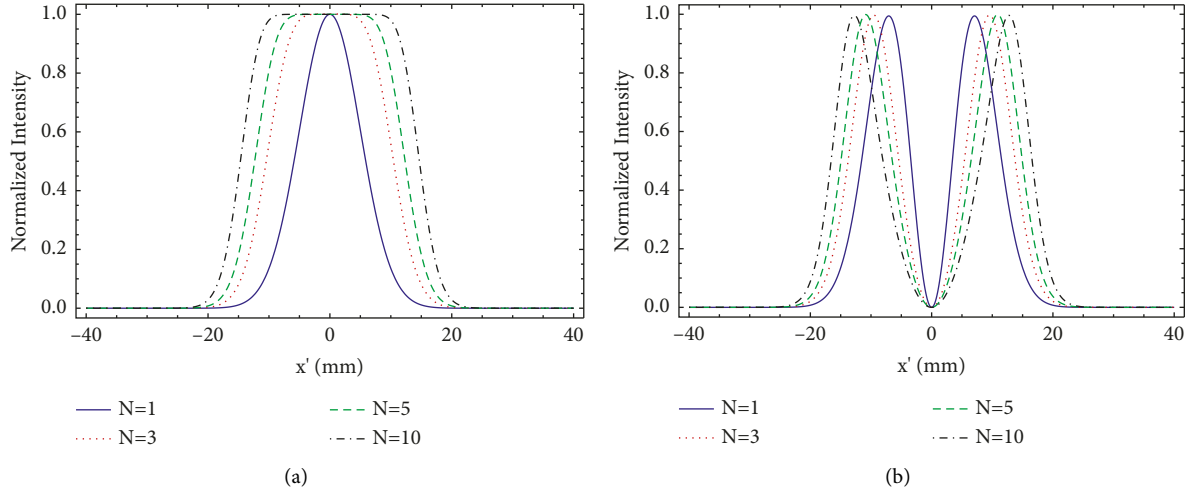
FIGURE 2: Normalized intensity distribution at the source plane before beam passing through anisotropic turbulent plasma for $w_0 = 1$ cm. (a) Circular flat-topped nonvortex beam and (b) circular flat-topped vortex hollow beam.

$$E(\mathbf{r}\prime, 0) = \sum_{n=1}^{N} \frac{(-1)^{n-1}}{N} \frac{N!}{n!(N-n)!}$$

$$\exp\left[-n\left(\frac{x'^2 + y'^2}{w_0^2}\right)\right]\left(\frac{x\prime + iy\prime}{w_0}\right)^l, \tag{7}$$

where $\mathbf{r}\prime = (x\prime, y\prime)$ is the position vector at the source plane, N is the order of the circular flat-topped vortex hollow beam, w_0 denotes the beam width, and l is the topological charge. Figure 2(b) shows the normalized intensity distribution of the circular flat-topped vortex hollow beam for different values of N; when $l = 0$, Equation (7) will reduce to the electric field of a flat-topped nonvortex beam (Figure 2(a)).

The cross-spectral density characterizes the spatial correlations of the field at pairs of points $\mathbf{r}_1'$ and $\mathbf{r}_2'$ at the source plane and can be defined as follows [27]:

$$W(\mathbf{r}_1', \mathbf{r}_2', 0) = \langle E(\mathbf{r}_1', 0)E^*(\mathbf{r}_2', 0)\rangle,$$
$$= A(\mathbf{r}_1')A(\mathbf{r}_2')g(\mathbf{r}_1' - \mathbf{r}_2'), \tag{8}$$

where $E(\mathbf{r}_i', 0)$ is the electric field of a fully coherent optical vortex beam and $\mathbf{r}_i'$ is the position vector at the source plane, $i = 1, 2$. The angular brackets denote an ensemble average, while the asterisk $*$ denotes the complex conjugate, $A(\mathbf{r}_i')$ represents the amplitude, and $g(\mathbf{r}_1' - \mathbf{r}_2')$ denotes the correlation function between two points $\mathbf{r}_1'$ and $\mathbf{r}_2'$, which can be expressed as follows [27]:

$$g(\mathbf{r}_1' - \mathbf{r}_2') = \exp\left[-\frac{(\mathbf{r}_1' - \mathbf{r}_2')^2}{2\sigma^2}\right], \tag{9}$$

where σ denotes the spatial coherence length. Then the cross-spectral density of a partially coherent flat-topped vortex hollow beam of circular symmetry at the source plane can be calculated as follows:

$$W(\mathbf{r}_1', \mathbf{r}_2', 0) = \sum_{m=1}^{N} \sum_{n=1}^{N} \frac{(-1)^{m+n}}{N^2} \frac{N!}{m!(N-m)!} \frac{N!}{n!(N-n)!}$$

$$\exp\left[-m\left(\frac{x_1'^2 + y_1'^2}{w_0^2}\right) - n\left(\frac{x_2'^2 + y_2'^2}{w_0^2}\right)\right]$$

$$\times\left(\frac{x_1' + iy_1'}{w_0}\right)^l\left(\frac{x_2' - iy_2'}{w_0}\right)^l\exp\left[-\frac{(\mathbf{r}_1' - \mathbf{r}_2')^2}{2\sigma^2}\right]. \tag{10}$$

By using the extended Huygens–Fresnel integral formula, the cross-spectral density of the partially coherent circular flat-topped vortex hollow beam in anisotropic turbulent plasma can be expressed as follows [25, 28]:

$$W_{\text{out}}(\mathbf{r}_1, \mathbf{r}_2, z) = \left(\frac{k}{2\pi z}\right)^2 \iint W_{\text{in}}(\mathbf{r}_1', \mathbf{r}_2', 0)$$

$$\exp\left\{-\frac{ik}{2z}\left[(\mathbf{r}_1 - \mathbf{r}_1')^2 - (\mathbf{r}_2 - \mathbf{r}_2')^2\right]\right\}$$

$$\times \langle \exp\left[\psi^*(\mathbf{r}_1', \mathbf{r}_1, z) + \psi(\mathbf{r}_2', \mathbf{r}_2, z)\right]\rangle d^2 r_1' d^2 r_2', \tag{11}$$

where ψ is the random part of the complex phase of a spherical wave propagating through anisotropic turbulent plasma. Over the ensemble of the statistical realization of the random medium, we can write the equation as follows [29]:

$$\langle \exp\left[\psi^*((\mathbf{r}_1', \mathbf{r}_1, z) + \psi(\mathbf{r}_2', \mathbf{r}_2, z)\right]\rangle = \exp\left[-\frac{D_\psi(\mathbf{r}_1' - \mathbf{r}_2')}{2}\right]$$

$$\simeq -D_{sp}(z)\left[(\mathbf{r}_1 - \mathbf{r}_2)^2 + (\mathbf{r}_1 - \mathbf{r}_2)(\mathbf{r}_1' - \mathbf{r}_2') + (\mathbf{r}_1' - \mathbf{r}_2')^2\right], \tag{12}$$

where J_0 is the zero-order Bessel function and $D_\psi(\mathbf{r}_1' - \mathbf{r}_2')$ is the wave structure function through anisotropic turbulent plasma, which is given in Equation (1). Now, substituting Equations (10) and (12) into Equation (11), we get

$$
W_{\text{out}}(\mathbf{r}_1, \mathbf{r}_2, z) = \left(\frac{k}{2\pi z}\right)^2 \sum_{m=1}^{N} \sum_{n=1}^{N} \frac{(-1)^{m+n}}{N^2} \frac{N!}{m!(N-m)!} \frac{N!}{n!(N-n)!}
$$

$$
\iint \exp\left[-m\left(\frac{x_1'^2 + y_1'^2}{w_0^2}\right) - n\left(\frac{x_2'^2 + y_2'^2}{w_0^2}\right)\right]
$$

$$
\times \left(\frac{x_1' + iy_1'}{w_0}\right)^l \left(\frac{x_2' - iy_2'}{w_0}\right)^l \exp\left[-\frac{(\mathbf{r}_1' - \mathbf{r}_2')^2}{2\sigma^2}\right]
$$

$$
\exp\left\{-\frac{ik}{2z}\left[(\mathbf{r}_1 - \mathbf{r}_1')^2 - (\mathbf{r}_2 - \mathbf{r}_2')^2\right]\right\}
$$

$$
\times \exp\left\{-D_{sp}(z)\left[(\mathbf{r}_1 - \mathbf{r}_2)^2 + (\mathbf{r}_1 - \mathbf{r}_2)(\mathbf{r}_1' - \mathbf{r}_2')\right.\right.
$$

$$
\left.\left. + (\mathbf{r}_1' - \mathbf{r}_2')^2\right]\right\} d^2\mathbf{r}_1' d^2\mathbf{r}_2', \tag{13}
$$

Since the optical intensity of the partially coherent light is given by $I(\mathbf{r}, z) = W(\mathbf{r}, \mathbf{r}, z)$ [27], then the optical intensity of a partially coherent circular flat-topped vortex hollow beam can be written as

$$
I_{\text{out}}(\mathbf{r}, z) = \left(\frac{k}{2\pi z}\right)^2 \sum_{m=1}^{N} \sum_{n=1}^{N} \frac{(-1)^{m+n}}{N^2} \frac{N!}{m!(N-m)!} \frac{N!}{n!(N-n)!}
$$

$$
\iint \exp\left[-m\left(\frac{x_1'^2 + y_1'^2}{w_0^2}\right) - n\left(\frac{x_2'^2 + y_2'^2}{w_0^2}\right)\right]
$$

$$
\times \left[\frac{x_1'x_2' + y_1'y_2' + i(x_2'y_1' - x_1'y_2')}{w_0^2}\right]^l
$$

$$
\exp\left[-\frac{(\mathbf{r}_1' - \mathbf{r}_2')^2}{2\sigma^2}\right] \exp\left\{-\frac{ik}{2z}\left[(\mathbf{r} - \mathbf{r}_1')^2 - (\mathbf{r} - \mathbf{r}_2')^2\right]\right\}
$$

$$
\times \exp\left[-D_{sp}(z)(\mathbf{r}_1' - \mathbf{r}_2')^2\right] d^2\mathbf{r}_1' d^2\mathbf{r}_2',
$$

$$\tag{14}$$

Using the following expression [30], we get

$$
(x + iy)^n = \sum_{t=0}^{n} \frac{n!}{t!(n-t)!} x^{n-t} (iy)^t, \tag{15}
$$

and by applying the integral formula [31], we derive the following equation:

$$
\int_{-\infty}^{\infty} x^n \exp\left(-px^2 + 2qx\right) dx
$$

$$
= n! \sqrt{\frac{\pi}{p}} \left(\frac{q}{p}\right)^n \exp\left(\frac{q^2}{p}\right) \sum_{k=0}^{[n/2]} \frac{1}{k!(n-2k)!} \left(\frac{p}{4q^2}\right)^k. \tag{16}
$$

Using the following expression for the Hermite function $H_q(x)$ [30], we get

$$
H_n(x) = \sum_{k=0}^{[n/2]} \frac{(-1)^k n!}{k!(n-2k)!} (2x)^{n-2k}. \tag{17}
$$

The integration in Equation (14) can be evaluated, and finally, we obtain

$$
I_{\text{out}}(\mathbf{r}, z) = \left(\frac{k}{2\pi z}\right)^2 \sum_{m=1}^{N} \sum_{n=1}^{N} \frac{(-1)^{m+n}}{N^2} \frac{N!}{m!(N-m)!} \frac{N!}{n!(N-n)!}
$$

$$
\sum_{t=0}^{l} \frac{i^t l!}{t!(l-t)!} \left(\frac{1}{w0}\right)^l \sum_{s=0}^{l} \frac{(-i)^s l!}{s!(l-s)!} \left(\frac{1}{w0}\right)^l
$$

$$
\times \left\{ (l-t)! \sqrt{\frac{\pi}{a_1}} \left(\frac{1}{a_1}\right)^{l-t} \exp\left[-\frac{1}{a_1}\left(\frac{k}{2z}x\right)^2\right] \right.
$$

$$
\sum_{d_1=0}^{(l-t/2)} \frac{1}{d_1!(l-t-2d_1)!} \left(\frac{a_1}{4}\right)^{d_1} \sum_{t_1=0}^{l-t-2d_1} \frac{(l-t-2d_1)!}{t_1!(l-t-2d_1-t_1)!}
$$

$$
\times \left(\frac{ik}{2z}x\right)^{l-t-2d_1-t_1} \left(\frac{1}{2\sigma^2} + D_{sp}(z)\right)^{t_1} 2^{-l+s-t_1} i^{l-s+t_1} \tag{18}
$$

$$
\exp\left(\frac{c_1^2}{b_1}\right) \sqrt{\frac{\pi}{b_1}} \left(\frac{1}{\sqrt{b_1}}\right)^{l-s+t_1} H_{l-s+t_1}\left(-i\frac{c_1}{\sqrt{b_1}}\right) \bigg\}
$$

$$
\times \left\{ (t)! \sqrt{\frac{\pi}{a_2}} \left(\frac{1}{a_2}\right)^{t} \exp\left[-\frac{1}{a_2}\left(\frac{k}{2z}y\right)^2\right] \right.
$$

$$
\sum_{d_2=0}^{(t/2)} \frac{1}{d_2!(t-2d_2)!} \left(\frac{a_2}{4}\right)^{d_2} \sum_{t_2=0}^{t-2d_2} \frac{(t-2d_2)!}{t_2!(t-2d_2-t_2)!} \left(\frac{ik}{2z}y\right)^{t-2d_2-t_2}
$$

$$
\times \left(\frac{1}{2\sigma^2} + D_{sp}(z)\right)^{t_2} 2^{-s-t_2} i^{s+t_2}
$$

$$
\exp\left(\frac{c_2^2}{b_2}\right) \sqrt{\frac{\pi}{b_2}} \left(\frac{1}{\sqrt{b_2}}\right)^{s+t_2} H_{s+t_2}\left(-i\frac{c_2}{\sqrt{b_2}}\right) \bigg\}.
$$

Equation (18) is the analytical expression of the optical intensity of the partially coherent circular FT vortex hollow beam in anisotropic plasma turbulence, where

$$
a_1 = a_2 = \frac{n}{w_0^2} + \frac{1}{2\sigma^2} + \frac{ik}{2z} + D_{sp}(z),
$$

$$
b_1 = b_2 = \frac{m}{w_0^2} + \frac{1}{2\sigma^2} - \frac{ik}{2z} + D_{sp}(z) - \frac{1}{a_1}\left[\frac{1}{2\sigma^2} + D_{sp}(z)\right]^2,
$$

$$
c_1 = \frac{1}{a_1}\left[\frac{1}{2\sigma^2} + D_{sp}(z)\right]\frac{ik}{2z}x - \frac{ik}{2z}x,
$$

$$
c_2 = \frac{1}{a_1}\left[\frac{1}{2\sigma^2} + D_{sp}(z)\right]\frac{ik}{2z}y - \frac{ik}{2z}y.
$$

$$\tag{19}$$
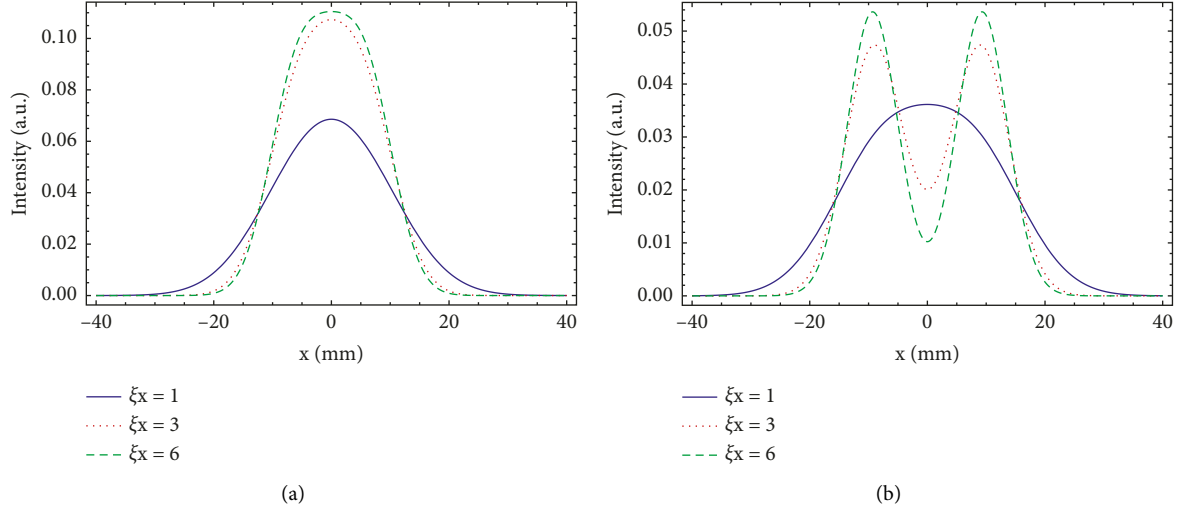
FIGURE 3: Cross-sections of the intensity distribution of the partially coherent circular: (a) flat-topped nonvortex beam and (b) flat-topped vortex hollow beam in anisotropic turbulent plasma for different values of the anisotropy parameter ξ_x ($z = 1m$).
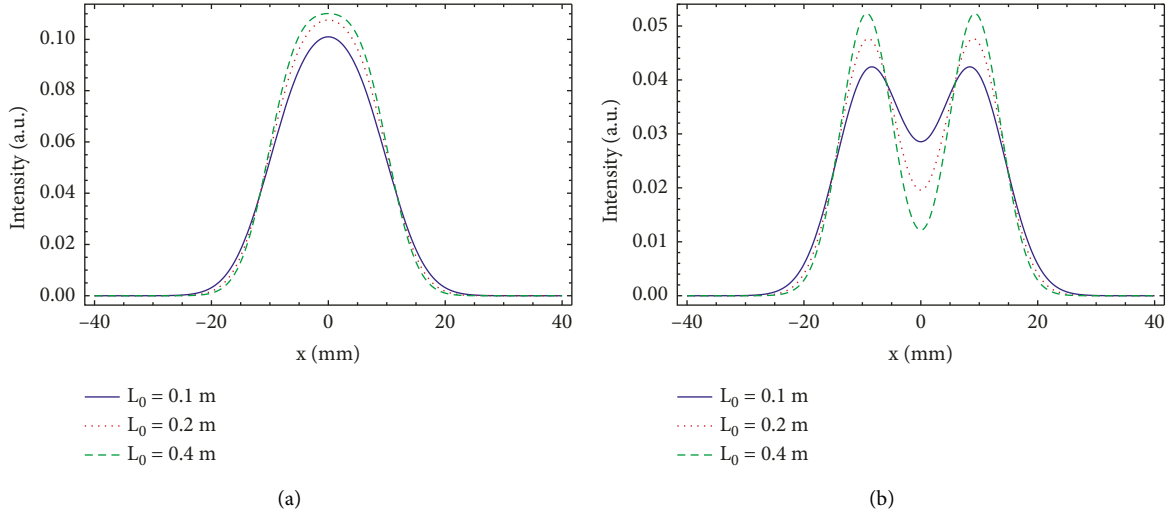
FIGURE 4: Cross-sections of the intensity distribution of the partially coherent circular: (a) flat-topped nonvortex beam and (b) flat-topped vortex hollow beam in anisotropic turbulent plasma for different values of the outer scale L_0 ($z = 1m$).

4. Numerical Results and Discussion

In this section, we numerically investigate the effects of the source and turbulent plasma parameters on the evolution properties of partially coherent circular FT vortex hollow and nonvortex beams and the comparison of the intensity distribution versus the propagation distance between partially coherent circular FT vortex hollow and non-vortex beams in anisotropic turbulent plasma. The beam parameters are taken as follows (unless the other values of parameters are specified in the figure): the order of the circular FT beam $N = 3$, the topological charge for the vortex hollow beam $l = 1$ and nonvortex beam $l = 0$, the beam width $w_0 = 1cm$, the wavelength $\lambda = 1550nm$, and the spatial coherence length $\sigma = 1mm$, whereas the anisotropic turbulent plasma parameters are taken as follows: the outer and inner scales of the turbulence $L_0 = 0.1m$ and $l_0 = 5 \times 10^{-6}m$,

respectively, the refractive index fluctuation variance $\langle n_1^2 \rangle = 0.73 \times 10^{-20}$, and anisotropy parameters $\xi_x = 2$, $\xi_y = 1$ [24].

4.1. The Effects of the Turbulent Plasma Parameters on Beam Evolution. Figures 3–5 have presented the intensity distribution of partially coherent FT vortex hollow/nonvortex beams under the influence of anisotropic turbulent plasma parameters. From Figure 3, we can see that by increasing the anisotropic parameter ξ_x, the axial intensity distribution of both nonvortex and vortex hollow beams increases, while the beam size becomes narrower as shown in Figures 3(a) and 3(b). The intensity distribution in Figure 3(a) shows a circular FT beam profile evolving into a Gauss-like beam as a result of the decreasing anisotropy parameter ξ_x, and from Figure 3(b), it can be seen that decreasing the anisotropy
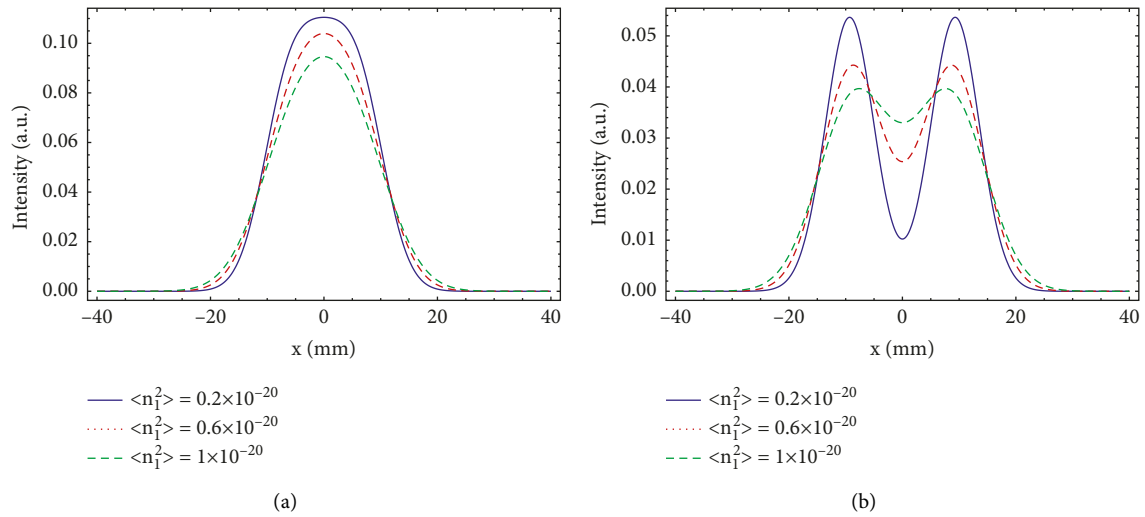
FIGURE 5: Cross-sections of the intensity distribution of the partially coherent circular: (a) flat-topped nonvortex beam and (b) flat-topped vortex hollow beam in anisotropic turbulent plasma for different values of the refractive index fluctuation variance $\langle n_I^2 \rangle$ ($z = 1$m).
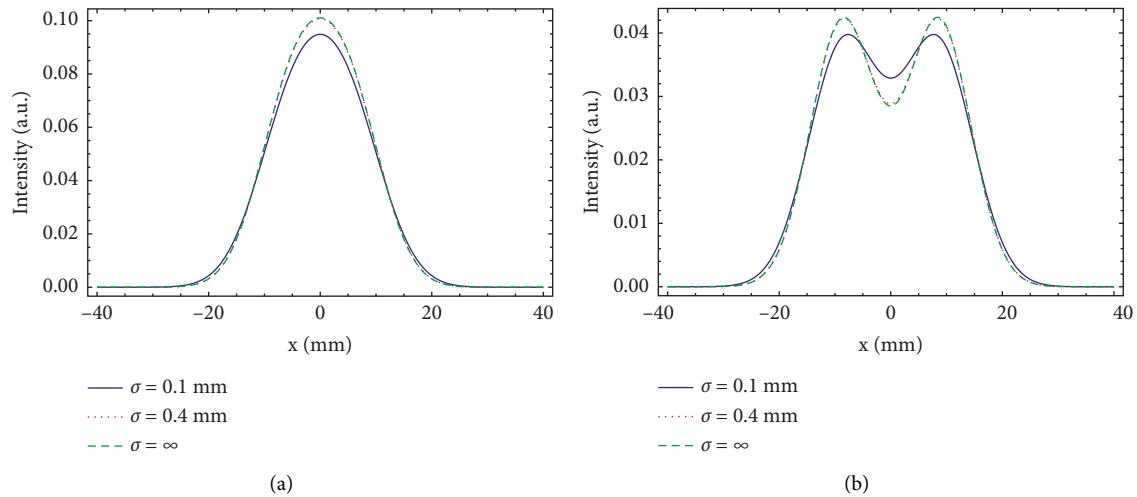
FIGURE 6: Cross-sections of the intensity distribution of the partially coherent circular: (a) flat-topped nonvortex beam and (b) flat-topped vortex hollow beam in anisotropic turbulent plasma for different values of the spatial coherence length σ ($z = 1$m).
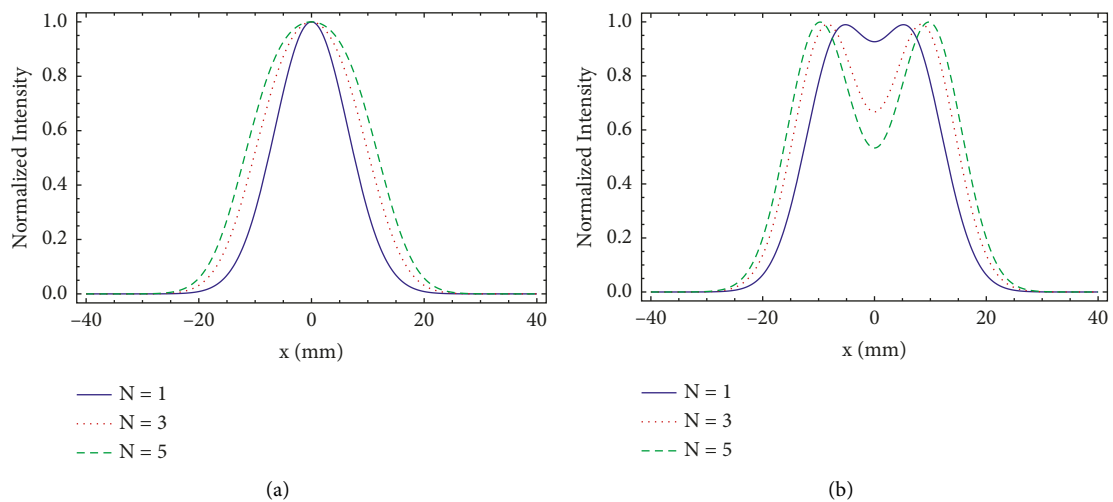
FIGURE 7: Cross-sections of the intensity distribution of the partially coherent circular: (a) flat-topped nonvortex beam and (b) flat-topped vortex hollow beam in anisotropic turbulent plasma for different values of the order of the circular flat-topped beam N ($z = 1$m).
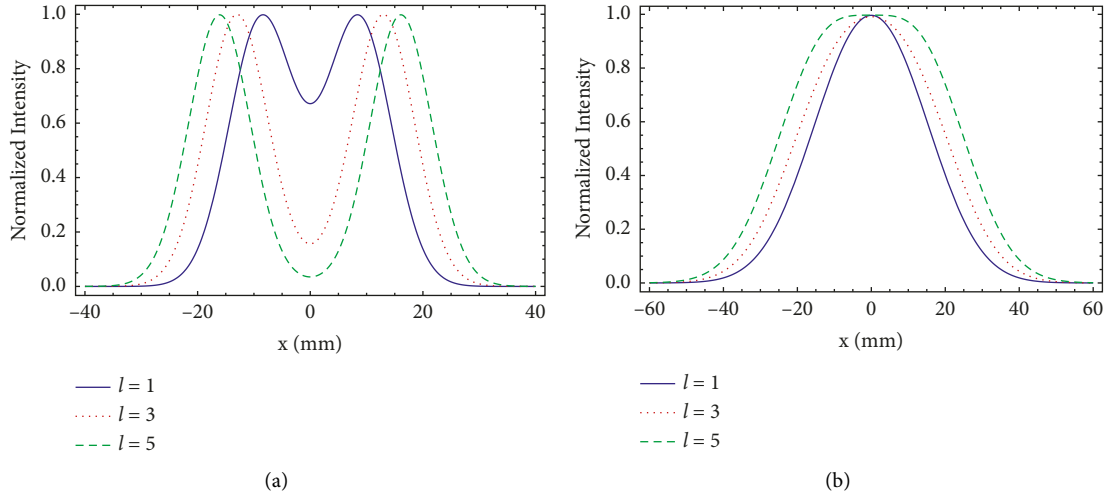
FIGURE 8: Cross-sections of the intensity distribution of the partially coherent circular flat-topped vortex hollow beam in anisotropic turbulent plasma for different values of the topological charge l at (a)$z = 1$m and (b)$z = 2$m.
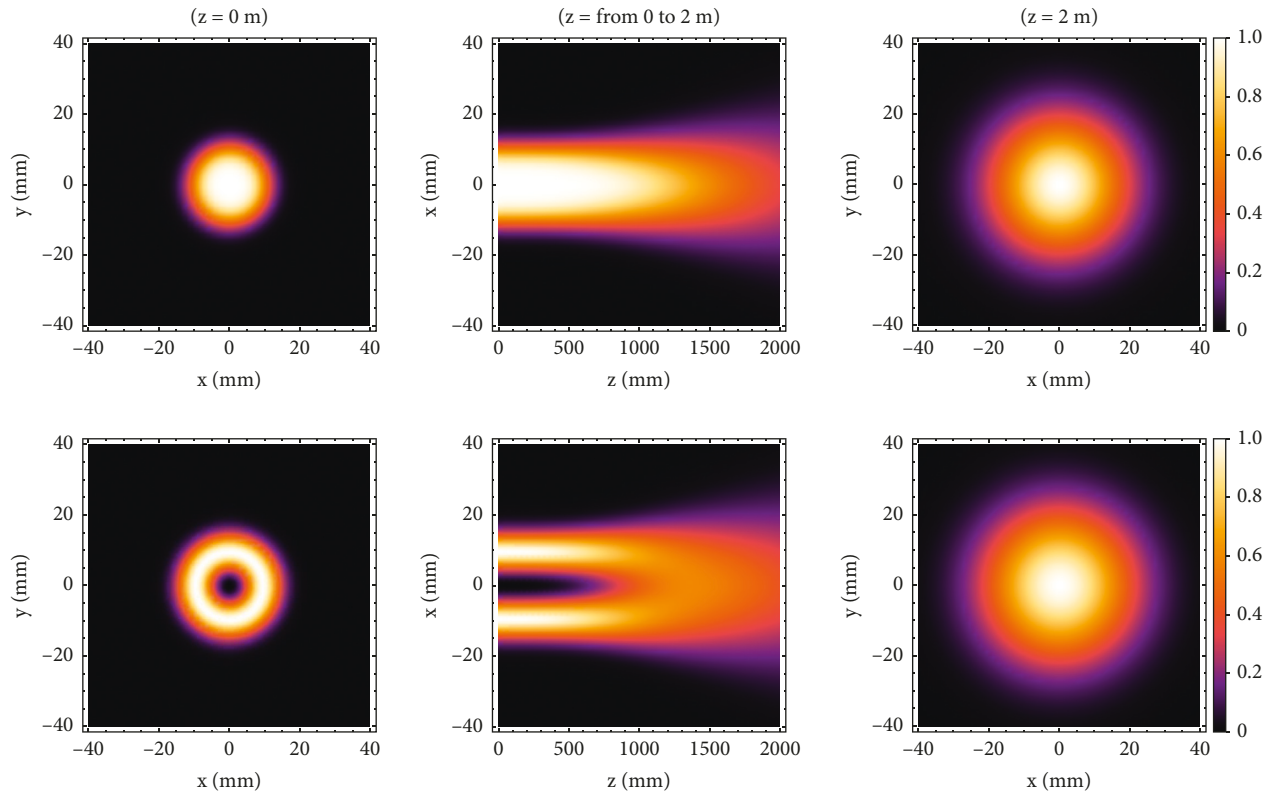
FIGURE 9: The intensity distribution of the partially coherent circular flat-topped nonvortex beam (top row) and vortex hollow beam (bottom row) in anisotropic turbulent plasma for different values of propagation distances z.

parameter ξ_x leads to a decrease in the dark hollow center of the vortex hollow beam; the profile of the partially coherent FT vortex hollow beam evolves into the Gauss-like beam for the lower value of ξ_x. These results indicate that the anisotropy in turbulent plasma reduces the turbulence effect on the evolution behavior of intensity distribution.

Figure 4 shows the variations of the partially coherent FT nonvortex and vortex hollow beams in anisotropic turbulent plasma for different values of the outer scale of the plasma turbulence L_0. It is observed that the profiles of partially coherent FT nonvortex and vortex hollow beams become smaller with increasing L_0, while the axial intensity drops as L_0 decreases as shown in Figures 3(a) and 3(b). We can see
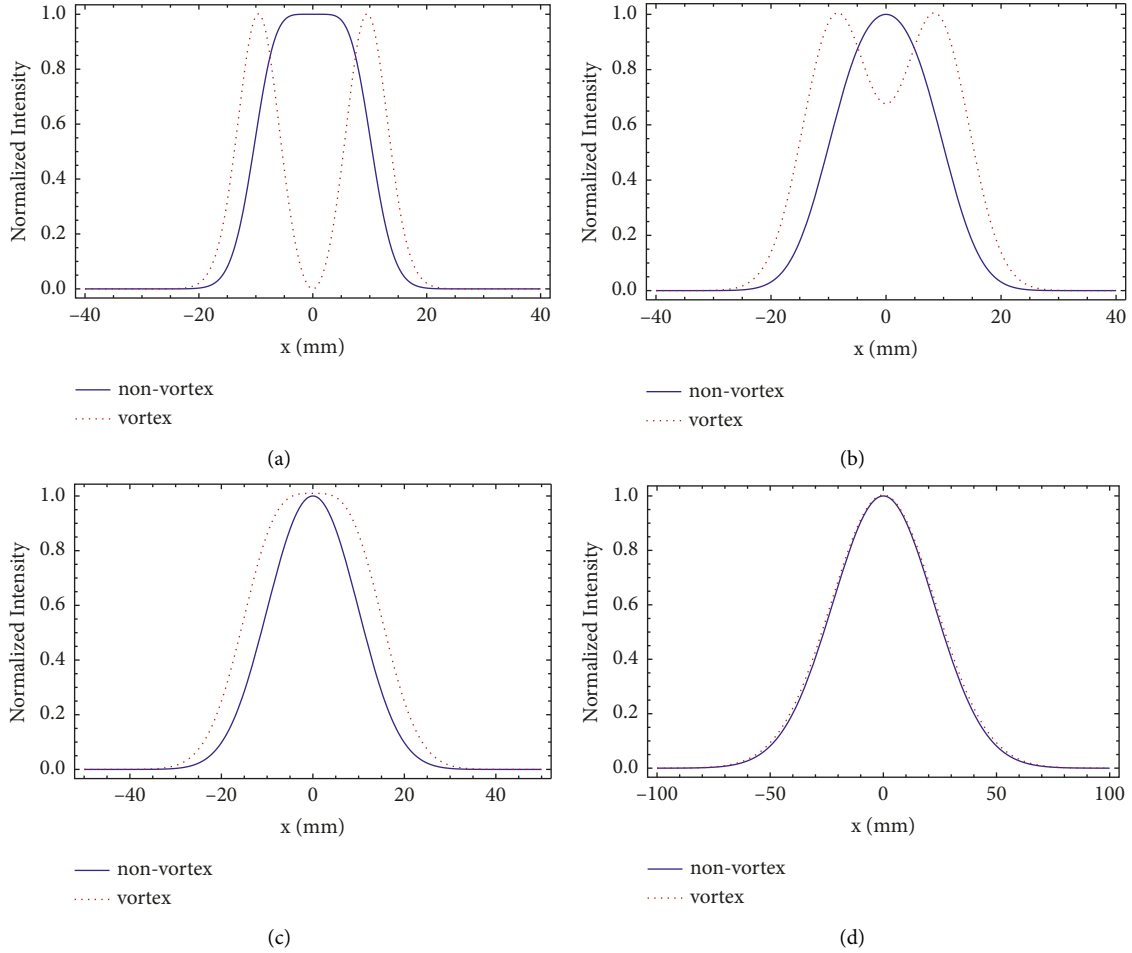
FIGURE 10: The normalized intensity distribution of the partially coherent circular FT vortex hollow beam and FT nonvortex beam in anisotropic turbulent plasma for different values of propagation distances: (a)$z = 0$m, (b)$z = 1$m, (c)$z = 1.3$m, and (d)$z = 3$m.

from Figure 4(a) that the intensity distribution profile for a circular flat-topped beam evolves into a Gauss-like beam with the decrease of L_0. For a partially coherent FT vortex hollow beam, Figure 4(b) indicates that when the outer scale of the turbulence enlarges, the dark hollow center of the beam increases.

Figures 5(a) and 5(b) show the partially coherent FT vortex hollow and nonvortex beam in anisotropic turbulent plasma for different values of the variance of the refractive index $\langle n_1^2 \rangle$. From these figures, we can see that the axial intensity drops as $\langle n_1^2 \rangle$ increases, and the beam size (FT nonvortex and FT vortex hollow beams) becomes wide. The intensity distribution in Figure 5(a) presents a circular flat-topped beam profile that evolves into a Gauss-like beam as a result of increasing the variance of the refractive index $\langle n_1^2 \rangle$. One can see from Figure 5(b) that for a small variance of the refractive index $\langle n_1^2 \rangle$, the intensity distribution retains a dark hollow pattern. In this case, the effect of turbulent plasma on the beam is not noticeable, while for a large variance of the refractive index $\langle n_1^2 \rangle$, the influence of the variance of the refractive index $\langle n_1^2 \rangle$ on the propagation of the beam becomes more noticeable, and the profile of the

hollow intensity is destroyed and becomes Gaussian distribution.

4.2. The Effects of the Source Parameters on Beam Evolution.
Figures 6 and 7 present the modifications on the intensity distribution of partially coherent FT vortex hollow and nonvortex beams under the influence of the source parameters. To investigate the influences of spatial coherence length σ on the spreading properties of partially coherent FT nonvortex and vortex hollow beams, the cross-sections of the intensity distribution of partially coherent FT nonvortex and vortex hollow beams propagating in anisotropic turbulent plasma for different values of the spatial coherence length σ are given in Figure 6. From Figures 6(a) and 6(b), we can see that the axial intensity drops as σ decreases, while the beam size does not change. As shown in Figure 6(b), increasing the spatial coherence length σ increases the dark hollow center of the partially coherent FT vortex hollow beam. Therefore, when the partially coherent FT vortex hollow beam propagates in anisotropic turbulent plasma, the change of the intensity distribution is affected by the spatial coherence of the source.

Figure 7 shows the cross-sections of the intensity distribution of partially coherent circular FT nonvortex and vortex hollow beams for different values of the order of the circular flat-topped beam N. From Figures 7(a) and 7(b), we can see that the beam size becomes wider with the increase in N, and it is found that the partially coherent circular nonvortex and vortex hollow beams with larger orders of the circular flat-topped beam can keep the beam profile better when the beam propagates in turbulent plasma. From Figure 7(b), it is seen that increasing N can increase the dark hollow center of the FT vortex hollow beam.

Figure 8 show cross-sections of normalized intensities for partially coherent circular flat-topped vortex hollow beams propagating through turbulent plasma for the different topological charge l. As can be seen, the beam with larger l has the larger dark hollow center in the near field (Figure 8(a)), and the beam with the different l will evolve into a Gauss-like beam with an increase in the propagation distance (Figure 8(b)) due to the influence of turbulent plasma. It can be noted that the beam with larger l will lose its initial dark hollow center slowly.

4.3. The Comparison of the Intensity Distribution versus the Propagation Distance. From Figure 9, we can see that the intensity of both partially coherent FT nonvortex and vortex hollow beams gradually decreases and becomes weaker with increasing propagation distance z, and also, one can find that the beam significantly expands during the propagation. For comparison, the corresponding results of partially coherent flat-topped nonvortex and vortex hollow beams are shown together propagating in anisotropic turbulent plasma for different values of propagation distance z as shown in Figure 10. From Figures 10(a)–10(d), as can be seen, the partially coherent flat-topped vortex hollow beam propagating in turbulent plasma can keep its initial dark center at a short propagation distance (Figure 10(a)). As the propagation distance z increases, the beam will lose its initial dark center and evolve into a Gaussian-like beam. The reason for this phenomenon is that as the transmission distance of the dark hollow center beam increases, the dark hollow center beam expands due to turbulence and diffraction, among which the expansion towards the center of the dark hollow causes the spot center to breakdown. It is worth noting that a general optical beam will finally converge into a Gaussian intensity profile at increasing propagation distances, and this result is in a good agreement as shown by the authors in [32].

5. Conclusions

In this paper, the partially coherent circular FT vortex hollow/nonvortex beams propagating in anisotropic turbulent plasma have been investigated by using the extended Huygens–Fresnel diffraction integral. We have analyzed and discussed the dependence of the beam evolution on the anisotropic turbulent plasma parameters, source parameters, and the propagation distance by using numerical examples. It can be seen from our results that the partially coherent circular FT vortex hollow/nonvortex beams evolve into Gaussian-like beams because of a decrease in the anisotropy parameter ξ_x and outer scale L_0 or increase in the refractive index fluctuation variance $\langle n_1^2 \rangle$. It is found that when the beam propagates in anisotropic turbulent plasma, the partially coherent FT vortex hollow/nonvortex beams with high order N and topological charge l of the circular FT beam can keep the beam profile better. It is to be noted that these results may be useful for optical communications.

Data Availability

The extended Huygens–Fresnel integral that we applied to obtain the analytical expression of the optical intensity of beams in turbulent plasma is taken from reference [25]. The wave structure function of a spherical wave propagating in the anisotropic turbulent plasma is taken from previously reported studies, which have been cited in [24]. The analytical expression of the optical intensity of the partially coherent circular flat-topped vortex hollow beam in anisotropic plasma turbulence in Equation (18) is obtained by using the famous mathematical expressions and integral formula found in references [30, 31].

Disclosure

This research is based on a theoretical study of "Propagation of Partially Coherent Vortex beam in Anisotropic Turbulent Plasma," and it is the thesis of Ph.D. presented at Sana'a University, Yemen.

Conflicts of Interest

The authors declare that they have no conflicts of interest.

References

[1] S. C. H. Wang and M. A. Plonus, "Optical beam propagation for a partially coherent source in the turbulent atmosphere," *Journal of the Optical Society of America*, vol. 69, no. 9, pp. 1297–1304, 1979.

[2] J. C. Ricklin and F. M. Davidson, "Atmospheric turbulence effects on a partially coherent Gaussian beam: implications for free-space laser communication," *Journal of the Optical Society of America A*, vol. 19, no. 9, pp. 1794–1802, 2002.

[3] T. Shirai, A. Dogariu, and E. Wolf, "Mode analysis of spreading of partially coherent beams propagating through atmospheric turbulence," *Journal of the Optical Society of America A*, vol. 20, no. 6, pp. 1094–1102, 2003.

[4] J. T. Li and L. X. Guo, "Research on electromagnetic scattering characteristics of reentry vehicles and blackout forecast model," *Journal of Electromagnetic Waves and Applications*, vol. 26, no. 13, pp. 1767–1778, 2012.

[5] T. C. Lin and L. K. Sproul, "Influence of reentry turbulent plasma fluctuation on EM wave propagation," *Computers & Fluids*, vol. 35, no. 7, pp. 703–711, 2006.

[6] H. Ding, S. Yi, Y. Zhu, and L. He, "Experimental investigation on aero-optics of supersonic turbulent boundary layers," *Applied Optics*, vol. 56, no. 27, pp. 7604–7610, 2017.

[7] R. P. Starkey, "Hypersonic vehicle telemetry blackout analysis," *Journal of Spacecraft and Rockets*, vol. 52, no. 2, pp. 426–438, 2015.

[8] C. Lv, Z. Cui, and Y. Han, "Light propagation characteristics of turbulent plasma sheath surrounding the hypersonic aerocraft," *Chinese Physics B*, vol. 28, no. 7, Article ID 074203, 2019.

[9] J. Li, S. Yang, and L. Guo, "Propagation characteristics of Gaussian beams in plasma sheath turbulence," *IET Microwaves, Antennas & Propagation*, vol. 11, no. 2, pp. 280–286, 2017.

[10] J. Li, S. Yang, L. Guo, M. Cheng, and T. Gong, "Bit error rate performance of free-space optical link under effect of plasma sheath turbulence," *Optics Communications*, vol. 396, pp. 1–7, 2017.

[11] C. J. Lü and Y. P. Han, "Analysis of propagation characteristics of Gaussian beams in turbulent plasma sheaths," *Acta Physica Sinica*, vol. 68, no. 9, Article ID 094201, 2019.

[12] X. Huang, S. Nan, W. Tan, Y. Bai, and X. Fu, "Statistical properties of Gaussian Schell-model beams propagating through anisotropic hypersonic turbulence," *OSA Continuum*, vol. 2, no. 12, pp. 3584–3597, 2019.

[13] J. Li, J. Li, L. Guo, M. Cheng, and L. Xi, "Polarization characteristics of radially polarized partially coherent vortex beam in anisotropic plasma turbulence," *Waves in Random and Complex Media*, vol. 31, no. 6, pp. 1931–1944, 2021.

[14] L. Allen, M. W. Beijersbergen, R. J. C. Spreeuw, and J. P. Woerdman, "Orbital angular momentum of light and the transformation of Laguerre-Gaussian laser modes," *Physical Review A*, vol. 45, no. 11, pp. 8185–8189, 1992.

[15] B. Yan, Z. Lu, J. Hu et al., "Orbital angular momentum (OAM) carried by asymmetric vortex beams for wireless communications: theory, experiment and current challenges," *IEEE Journal of Selected Topics in Quantum Electronics*, vol. 27, no. 2, pp. 1–10, 2021.

[16] F. Gori, "Flattened Gaussian beams," *Optics Communications*, vol. 107, no. 5-6, pp. 335–341, 1994.

[17] H. Liu, Y. Lü, J. Xia, X. Pu, and L. Zhang, "Flat-topped vortex hollow beam and its propagation properties," *Journal of Optics*, vol. 17, no. 7, Article ID 075606, 2015.

[18] Z. Liu, J. Dai, X. Sun, and S. Liu, "Generation of hollow Gaussian beam by phase-only filtering," *Optics Express*, vol. 16, no. 24, Article ID 19926, 2008.

[19] Y. Li, "Light beams with flat-topped profiles," *Optics Letters*, vol. 27, no. 12, pp. 1007–1009, 2002.

[20] B. Lü, S. Luo, and B. Zhang, "Propagation of flattened Gaussian beams with rectangular symmetry passing through a paraxial optical ABCD system with and without aperture," *Optics Communications*, vol. 164, no. 1-3, pp. 1–6, 1999.

[21] Y. Cai, "Propagation of various flat-topped beams in a turbulent atmosphere," *Journal of Optics A: Pure and Applied Optics*, vol. 8, no. 6, pp. 537–545, 2006.

[22] D. Liu, Y. Wang, and H. Yin, "Evolution properties of partially coherent flat-topped vortex hollow beam in oceanic turbulence," *Applied Optics*, vol. 54, no. 35, Article ID 10510, 2015.

[23] F. M. Thabit, A. A. AlKelly, and M. A. Shukri, "Propagation of fully and partially coherent flat-topped multi-Gaussian beams through axicons," *Journal of the Optical Society of America A*, vol. 37, no. 5, pp. 759–767, 2020.

[24] J. Li, S. Yang, L. Guo, and M. Cheng, "Anisotropic power spectrum of refractive-index fluctuation in hypersonic turbulence," *Applied Optics*, vol. 55, no. 32, pp. 9137–9144, 2016.

[25] L. C. Andrews and R. L. Phillips, *Laser Beam Propagation through Random Media*, SPIE Press Bellingham, Bellingham, WA, USA, 2nd edition, 2005.

[26] A. N. Shahrbabaki, M. Bazazzadeh, M. D. Manshadi, and A. Shahriari, "Designing a fuzzy logic controller for the Reynolds number in a blowdown supersonic wind tunnel," *IEEE Aerospace Conference*, pp. 1–12, 2014.

[27] L. Mandel and E. Wolf, *Optical Coherence and Quantum Optics*, Cambridge University Press, Cambridge, UK, 1995.

[28] Y. Xianyang and F. Wenyu, "Properties of the rotation and mergence of twisted Gaussian schell model array beams propagating in turbulent biological tissues," *International Journal of Optics*, vol. 2022, Article ID 1157777, 9 pages, 2022.

[29] G. Gbur and E. Wolf, "Spreading of partially coherent beams in random media," *Journal of the Optical Society of America A*, vol. 19, no. 8, pp. 1592–1598, 2002.

[30] A. Jeffrey and H. Dai, *Handbook of Mathematical Formulas and Integrals*, Academic Press, Cambridge, MA, USA, 4th edition, 2008.

[31] I. S. Gradshteyn and I. M. Ryzhik, *Table of Integrals, Series and Products*, Academic Press, Cambridge, MA, USA, 7th edition, 2007.

[32] H. T. Eyyuboğlu, Y. Baykal, and E. Sermutlu, "Convergence of general beams into Gaussian intensity profiles after propagation in turbulent atmosphere," *Optics Communications*, vol. 265, no. 2, pp. 399–405, 2006.